

## Surface degradation of $\text{YBa}_2\text{Cu}_3\text{O}_{7-\delta}$ superconductors on exposure to air and humidity

Temel H. Büyüklimanli and Joseph H. Simmons

University of Florida, Gainesville, Florida 32611-2066

(Received 21 September 1990)

Surface modifications from exposure of  $\text{YBa}_2\text{Cu}_3\text{O}_{7-\delta}$  pellets and thin films of the 1:2:3 composition to ambient atmosphere and 85% relative humidity at 50°C were measured using x-ray photoelectron spectroscopy and scanning Auger electron multiprobe. Surface formation of  $\text{BaCO}_3$  and  $\text{Ba(OH)}_2$  was detected. The surface layer of the sintered pellets did not have any Cu after 48 h of moisture treatment. The degradation in the thin-film samples was substantially less. The rate of degradation appears to be controlled by grain-boundary diffusion.

### INTRODUCTION

Several studies have reported environmental effects on 1:2:3 superconductors.<sup>1-13</sup> X-ray photoelectron spectroscopy (XPS) has been widely used to determine the surface structure of these materials and to investigate the structures associated with the occurrence of superconductivity at liquid-nitrogen temperatures. However, since XPS is a surface-sensitive technique, the extension of results to the bulk structure requires a careful cleaning of surface adsorbates. This step is complicated by the formation of a surface reaction layer after exposure to the atmosphere. There is no generally accepted method for removing surface contamination. Many methods have been suggested, but each has serious drawbacks. For example, vacuum fracture commonly practiced in sample preparation for XPS studies has been criticized for enhancement of grain boundaries at the fracture surface leading to a Ba-rich layer<sup>14,15</sup> except for single crystals; low-energy ion milling *in situ* causes differential sputtering of the elements, especially oxygen, and leads to incorrect compound stoichiometries;<sup>14,16,17</sup> surface scraping with a diamond or steel file is the most often used method, yet suffers from the same grain-boundary exposure problem as sample fracture.<sup>14,16,18</sup> Heating the sample until the contaminants are evaporated seems to be the most reliable method for measurement of the bulk structure.<sup>16</sup> The study presented here addresses this surface contamination or degradation problem by analyzing the surface reaction layer formed on 1:2:3 pellets and films under normal and accelerated corrosion conditions.

### EXPERIMENTS

Two types of samples were used for comparison purposes: pressed pellets and rf sputtered thin films. Pellets were prepared from powders of  $\text{Y}_2\text{O}_3$  ( $< 10 \mu\text{m}$  in diameter),  $\text{BaCO}_3$  ( $1 \mu\text{m}$  in diameter), and  $\text{CuO}$  ( $< 800 \mu\text{m}$  in diameter).<sup>19</sup> The powders had a nominal purity level of 99.999% for  $\text{Y}_2\text{O}_3$  and  $\text{CuO}$  and 99.9% for  $\text{BaCO}_3$ . The [Y]:[Ba]:[Cu] molar ratio in the mixture was 1:2:3. These powders were mechanically mixed for 24 h to ensure homogeneity. Mixed powders were calcined in an  $\text{Al}_2\text{O}_3$

crucible at 950°C in air for 1 h. The powders were quenched in air and then ground with mortar and pestle. Calcination and grinding steps were repeated a second time. Pellets with an average height of 1.35 mm and average diameter of 4.85 mm were pressed from 0.1 g of calcined powder at 430 MPa in a laboratory press. The pellets were then sintered at 950°C for 1 h in an  $\text{Al}_2\text{O}_3$  combustion boat. They were cooled slowly to 600°C and annealed for 3 h in flowing oxygen followed by slow cooling to room temperature in flowing oxygen. Films several micrometers thick with no particular orientation were deposited on  $\text{SrTiO}_3$  substrates by rf sputtering using  $\text{Y}_2\text{O}_3$ ,  $\text{CuO}$ , and  $\text{BaF}_2$  targets. They were treated with water vapor followed by a dry oxygen anneal. Details of the preparation are given elsewhere.<sup>20</sup> Two pellet samples from the same batch and two films from the same deposition were prepared, and one of each was tested for superconductivity, while the surface of the other was examined in the corrosion study. All samples were of the 1:2:3 nominal composition and had  $T_c$  in the range 80–90 K. Samples were analyzed immediately after preparation, following an ambient air exposure of 18 days and after exposure to 85% relative humidity and 50°C in a humidity chamber. XPS measurements were performed on a Perkin Elmer Phi ESCA 5000 with pass energies at 17.9 and 8.95 eV and Mg x rays operated at 300 w. Angle-resolved measurements were also made on the same instrument between 15° and 80°. The typical binding-energy resolution was 1.4 eV full width at half maximum (FWHM). Sputter depth profiling using three-point differentiation and peak-to-peak measurements was conducted on a Perkin Elmer Phi 660 Scanning Auger electron multiprobe (SAM). The beam energy of the electrons and Ar ions was 10 and 3 keV, respectively. The ion-beam diameter was 1 mm, creating a  $\sim 100\text{-\AA}/\text{min}$  sputtering yield. Typical vacua in both instruments were near  $10^{-9}$  Torr. Comparisons were made between the XPS and SAM data. X-ray-irradiation damage was detected as reported before,<sup>21</sup> mostly as a reduction of oxygen content, leaving a more metallic surface after 50 min of irradiation. In order to minimize this effect during the measurements, fast data acquisitions were performed at the expense of higher resolution. Sam-

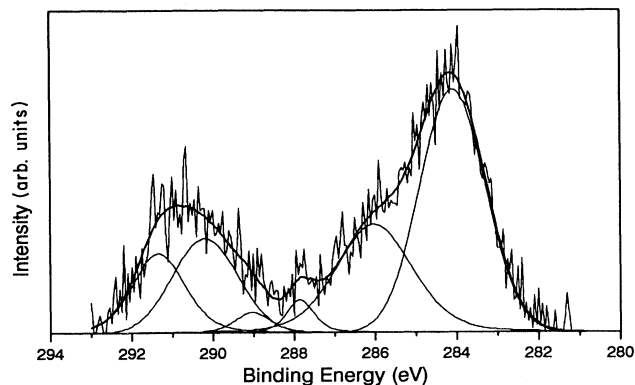


FIG. 1. C 1s XPS spectra from 1:2:3 pellet.

ples were analyzed without surface cleaning in order to examine the effect of the environment on the actual sample surface. XPS spectra of Ba 4d and 3d<sub>5/2</sub>, O 1s, Cu 2p<sub>3/2</sub>, Y 3d, and C 1s orbitals as well as x-ray-induced Auger transitions of Ba, O, and Cu were collected. For charge referencing the C 1s peak was used after curve fitting with six peaks (Fig. 1) and assigning the lowest binding-energy peak to hydrocarbon species. This peak was set to 284.6 eV.

### RESULTS AND DISCUSSION

The XPS analyses of fresh and exposed sample surfaces from the pellets and thin films are presented first. Figure 2 shows the relative changes in Ba and Cu atomic concentrations between various conditions of exposure [(a) freshly prepared, (b) following 18 days in ambient air, and following (c) 5, (d) 12, and (e) 48 h in a controlled-humidity chamber at 50°C with a relative humidity of 85%], on both the bulk sample pellet and thin film. Barium increases with respect to Cu both under ambient and humid air exposure. After exposure to humid environments, the Cu concentration decreases drastically in both samples and the superconductivity is quenched.

The concentration profiles of Cu, Ba, Y, O, and C were measured as a function of distance from the surface by both angle-resolved XPS and argon-ion-sputtered scanning Auger microprobe (SAM) measurements. Both approaches are subject to some limitations, and these are discussed below.

Angle-resolved XPS measurements have been reported by a variety of authors.<sup>18,22,23</sup> The results of this study clearly show an increase in Ba and O content and a decrease in Y and Cu content toward the surface. The Ba increase essentially agrees with other reports, which measured it with different techniques upon exposure to CO<sub>2</sub>, air, and moisture.<sup>3,7,12,22,24-28</sup> However, angle-resolved XPS studies require very smooth surfaces (i.e., the surface roughness must be less than the escape depth of the electrons).<sup>18</sup> This clearly was not the case in the pellet samples and was marginal in the thin-film samples. Therefore, only qualitative change in species concentration are possible with this method. Quantitative measurements of the depth profiles were obtained using

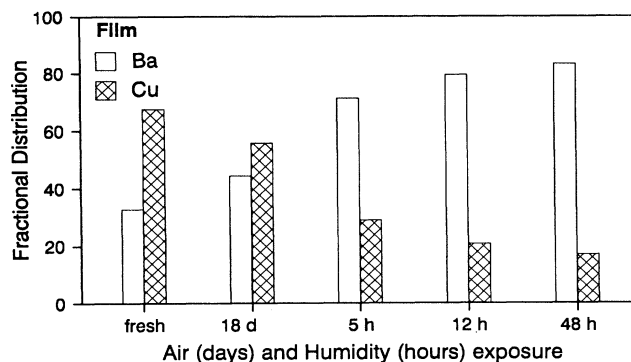
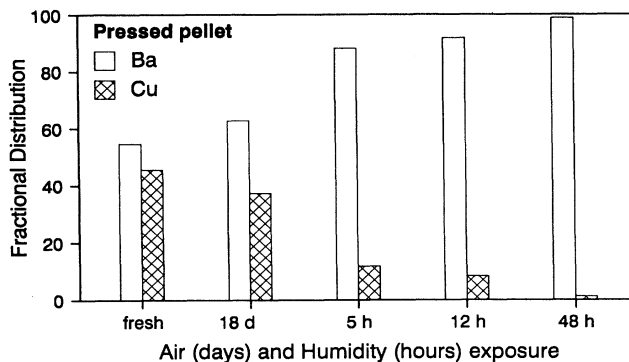


FIG. 2. Relative change of Ba and Cu atomic concentration during moisture treatment of 1:2:3 ceramics measured by integration of the Ba 3d<sub>5/2</sub> and Cu 2p<sub>3/2</sub> peaks in XPS.

argon-ion-sputtered SAM analysis. The argon-ion beam was adjusted to produce a sputtering rate of ~100 Å/min. In order to test for any occurrence of differential oxygen sputtering, data acquisition was continued well into the bulk, at which point the sputtering yield saturated and no further change in concentration of Ba, O, Y, or Cu was observed. This guaranteed that the overall sputtering rates were equivalent for the four components. A SAM trace of the depth profile in a freshly prepared pellet sample (Fig. 3) confirms these results as the relative

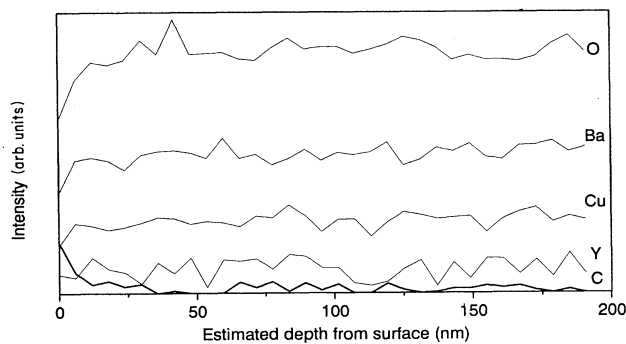


FIG. 3. Depth profile of fresh 1:2:3 pellet measured by SAM.

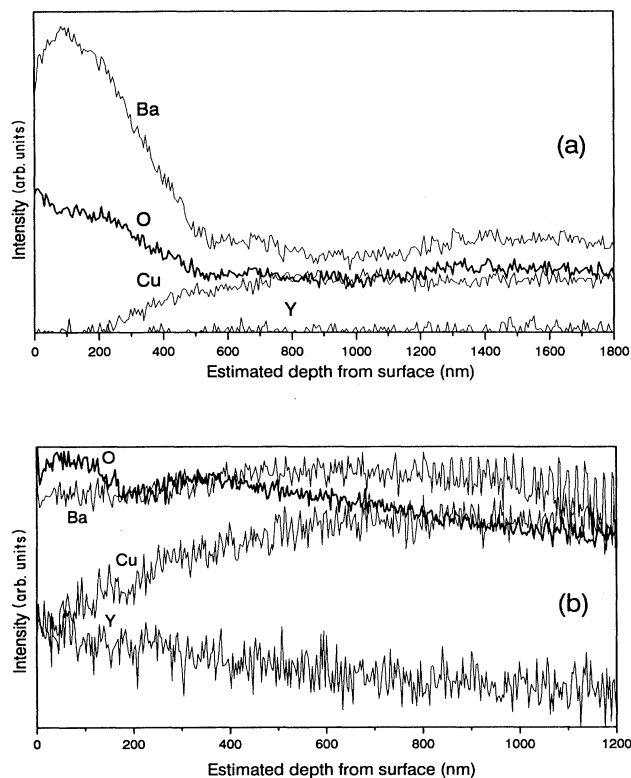


FIG. 4. Ion-assisted depth profile measured by SAM of the (a) sintered pellet and (b) rf sputtered film after 48 h at 85% relative humidity and 50°C.

peak intensities of each of the four components remain unchanged at depths greater than 200 nm. This is the same depth where large changes are observed in the exposed pellet.

Figure 4 shows peak-to-peak depth profiles in both the pellet and thin-film samples after a 48-h exposure to humidity. The data show a clear accumulation of Ba and O at the sample surfaces and a depletion of Cu for pressed powder. The intensity of Y was not adequate enough to make any judgement. The depletion and enrichment regions exhibit about the same thickness with Ba, Cu, Y, and O approaching their bulk concentrations at about 600 nm in the pellet sample. By contrast, the composition of the film was not as severely altered. The depth profile shows that there was no appreciable Ba enrichment and a much thinner Cu depletion layer [Fig. 4(b)]. As shown below, it was observed that formation of carbonates and hydroxyl groups and loss of superconducting component occur rapidly in pellets (Figs. 5 and 6). Such decompositions along the grain boundaries have been previously reported.<sup>7, 8, 10, 15, 18, 22, 29</sup>

The heats of formation of  $\text{Ba}(\text{OH})_2 \cdot 8\text{H}_2\text{O}$  (-798.8 kcal/mol),  $\text{BaO}_2 \cdot 8\text{H}_2\text{O}$  (-718.8 kcal/mol), and  $\text{BaC}_2\text{O}_4 \cdot 2\text{H}_2\text{O}$  (-471 kcal/mol) (Ref. 30) are strongly negative and consequently favor the formation of such compounds on the sample surface. The high diffusivity of Ba along the grain boundary provides the excess Ba to

fuel these reactions. A similar conclusion was obtained by others<sup>3, 25, 31</sup> based on the narrowing of the XPS Ba peak associated with release of oxygen in vacuum upon heating.<sup>16</sup> The result is further supported by the detection of nonsuperconducting Ba-containing phases at the grain boundaries.<sup>32</sup> Samples exposed to humidity were normally analyzed immediately. No changes were observed in Ba or O features when some samples were reanalyzed after they had been kept in UHV ( $10^{-9}$  Torr) overnight. We have also observed that in some cases carbonation of Ba occurs in high-stress areas, especially in pellets formed from pressed powders. Sequeira, Rajagopal, and Yakhmi<sup>2</sup> also conclude that nonsuperconducting amorphous phases formed at the grain boundaries were caused by strain fields and partial release of oxygen. Several studies have linked the degradation of 1:2:3 to oxygen defects in these materials.<sup>5, 13, 29</sup> In similar tests on higher-density pellets, we measured a less severe degradation while porous laser-ablated films showed much greater degradation in moist air. These results further support the speculation that the structure and size of the grain boundary (or grain) plays an important role in the resistance to degradation in humid air. Zandbergen,

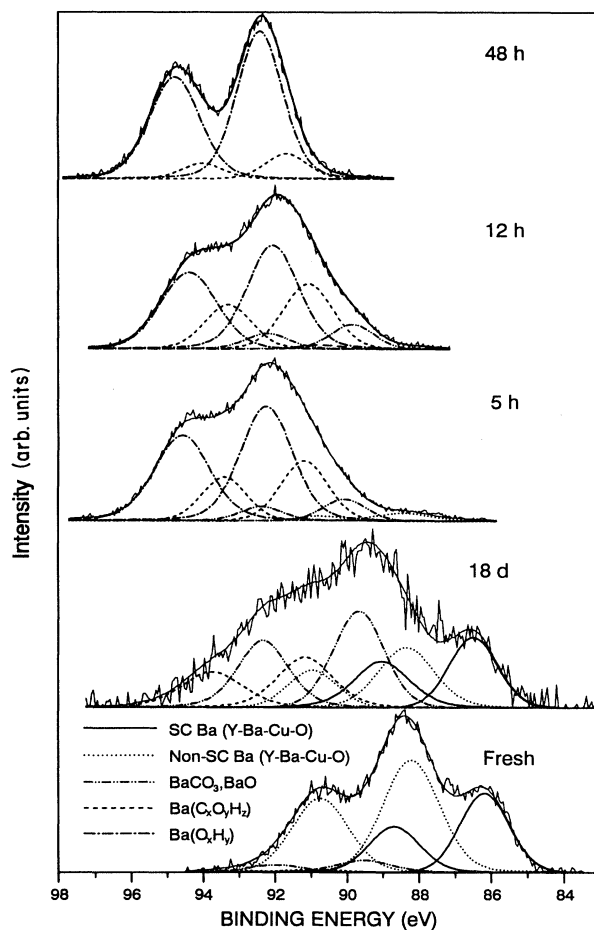


FIG. 5. Ba 4d spectra of the 1:2:3 pellet after exposure.

Gronsky, and Thomas<sup>5</sup> have demonstrated by means of transmission electron microscopy that defect-rich regions decomposed more rapidly.

XPS analysis of the surface can also yield information about chemical changes occurring with various degrees of exposure by means of chemical shift analysis of the deconvoluted peaks. The O 1s and Ba 4d peaks were deconvoluted into a series of components, closely matching the binding-energy positions reported in Ref. 22, except for the superconducting cuprate species in Ba 4d. An additional component which grew after exposure to humidity was identified as due to hydroxyl forms of Ba. The binding energies (BE) and component species assignments are shown in Tables I and II for the Ba 4d and O 1s XPS peaks. Studies by Ford *et al.*,<sup>16</sup> in which the Ba and O XPS peaks were analyzed, interpreted the 531-eV peak as a combination of surface and bulk species. Most studies<sup>7,22,25</sup> associated the peak with BaO<sub>2</sub> or BaCuO<sub>2</sub>

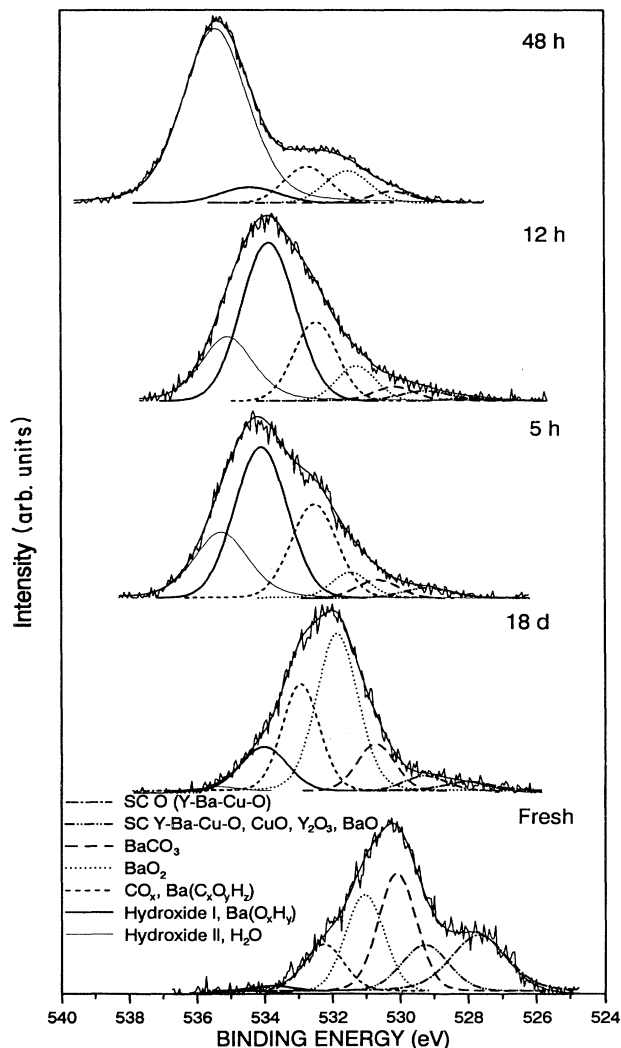


FIG. 6. O 1s spectra of the 1:2:3 pellet after exposure.

TABLE I. Components used to curve fit Ba 4d spectra of 1:2:3 compounds.

Ba 4d <sub>5/2</sub> BE (eV)±0.2	Assignment
86.4	superconducting Ba (Y-Ba-Cu-O)
88.2	nonsuperconducting Ba (Y-Ba-Cu-O)
89.6	BaCO <sub>3</sub> , BaO
91.0	Ba(C <sub>x</sub> O <sub>y</sub> H <sub>z</sub> )
92.1	Ba(O <sub>x</sub> H <sub>y</sub> )

formed on the surface after heat treatment<sup>16</sup> and exposure to atmosphere.<sup>3,7</sup> The observations reported here show that the 531 line is still present after Cu is no longer detected on the surface, and therefore the assignment to BaO<sub>2</sub> is only the more appropriate as shown in Table II. The cuprate species have lower binding energies (528 and 529 eV) as shown in Table II. The hydroxide line was found to have a higher binding energy than predicted by previous authors.<sup>18,22,23</sup> The 543- and 535.6-eV lines increased with exposure to humidity and most probably correspond to Ba(OH)<sub>2</sub>, Ba(OH)<sub>2</sub>·8H<sub>2</sub>O, BaC<sub>2</sub>O<sub>4</sub>·2H<sub>2</sub>O, and/or molecular water.<sup>33</sup> The O 1s peaks often detected in the 531-534-eV range have been attributed to a multiplicity of forms of chemically and physically bound water on the surface. The chemisorbed and physisorbed oxygen and hydroxyl are also found in this range, making a clear interpretation difficult.<sup>4,34</sup> The high binding-energy O 1s peak in the La<sub>2</sub>CuO<sub>4+δ</sub> system was also attributed to water.<sup>33</sup> The possibility of the presence of BaC<sub>x</sub>O<sub>y</sub>H<sub>z</sub> in this study arose from the fact that carbon had a component at 292.1 eV, which is much higher than the reported BaCO<sub>3</sub> peak at 288.6±0.3 eV,<sup>24,31,35,36</sup> also observed in this study (Fig. 1). This carbon peak is most likely related to a hydroxyl or a water compound since these usually have higher binding energies. In light of these considerations, we agree with Qui *et al.*<sup>3</sup> that O dimerization assumptions<sup>37,38</sup> in high-temperature superconductors, which result from the observation of O 1s peaks in the range 531–535 eV at low temperatures, should be carefully examined since increasing temperatures can also lead to the removal of OH species. These different binding-energy speculations can only be resolved by water reaction of BaO<sub>2</sub> and BaCO<sub>3</sub> and identification by x-ray diffraction (XRD) and XPS. In making the assignments of Tables I and II, we made sure that no impurities were present which would interfere with our interpretations. Curve

TABLE II. Components used to curve fit O 1s spectra of 1:2:3 compounds.

BE(eV)±0.2	Assignment
528.0	SC O (Y-Ba-Cu-O)
529.0	SC O (Y-Ba-Cu-O), CuO, Y <sub>2</sub> O <sub>3</sub> , BaO
530.2	BaCO <sub>3</sub>
531.3	BaO <sub>2</sub>
532.5	CO <sub>x</sub> , Ba(C <sub>x</sub> O <sub>y</sub> H <sub>z</sub> )
534.0	hydroxide I, Ba(O <sub>x</sub> H <sub>y</sub> )
535.6	hydroxide II, H <sub>2</sub> O

fitting was performed using the second-derivative method<sup>39</sup> to identify the component peaks after subtraction of x-ray line shape (often called deconvolution). This allowed an accurate measure of the number of components present and their binding energies. While curve fitting different spectra, the binding-energy positions were kept within  $\pm 0.2$  eV of the values given in Tables I and II. The same FWHM was resolved for all peaks. 90% Gaussian and 10% Lorentzian curves were used with integral base-line subtraction. For the Ba analysis the  $4d$  orbital was used rather than the  $3d_{5/2}$  peak since the chemical shifts of the higher electronic state are greater. We found the  $4d$  spin states ( $\frac{5}{2}$  and  $\frac{3}{2}$ ) to be separated by 2.5 eV as measured on BaO and  $\text{BaCO}_3$  samples after low-energy ion-sputter cleaning. This close separation complicates peak deconvolution. For every Ba species it was necessary to use two peaks with 2.5-eV separation and the intensity of the  $4d_{5/2}$  peak was taken at 1.5 times the  $4d_{3/2}$  peak intensity as measured in the BaO and  $\text{BaCO}_3$  samples. These considerations are in close agreement with earlier reports.<sup>16,22,40</sup> The  $\text{Ba(OH)}_x$  species in this study had a larger binding energy than predicted by the same reports. Figures 5 and 6 show the deconvolution of the Ba  $4d$  and O  $1s$  peaks for the bulk sample under all cases of exposure studied. While many of the peak assignments in XPS studies are based on direct and indirect inference both in this paper and in most of the literature, the assignments shown in Tables I and II agree

well with those of other authors and are consistent with a wide variety of measurements.<sup>22,40</sup> Instances where we differ from the literature have been identified and justified by other measurements.

Figures 7 and 8 show the variation of different surface chemical species identified using Tables I and II as a function of exposure condition. In the decomposition of the Ba  $4d$  peak, two barium cuprate peaks have been identified. The first is associated with a superconducting bulk cuprate structure, and the second is a nonsuperconducting cuprate structure, often associated with a surface species. This assignment is consistent with several reports of XPS analysis on superconducting 1:2:3 compounds. Ambient air exposure causes a greater degradation of the two barium cuprate peaks in the pellet than in the film. In fact, the film shows an unexpected resistance to degradation in ambient air. Exposure to humid air, however, has a drastic effect on the pellet, and a 5-h exposure is sufficient to virtually eliminate the superconducting cuprate peak from the surface, with the rapid formation of barium carbonate and hydroxide. The film still has significant superconducting cuprate at the end of the experiment, and the predominant reacted Ba species is the nonsuperconducting cuprate rather than the hydroxide or carbonate compounds. This shows that the reaction with water remained localized to the surface of the film, possibly because of reduced diffusion of Cu to the interior and Ba to the surface. In fact, both the SAM

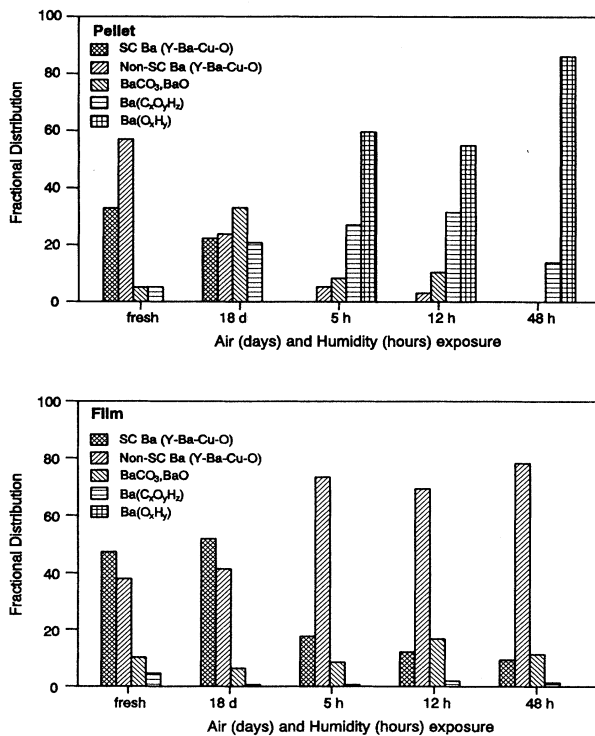


FIG. 7. Change in the Ba  $4d$  XPS peak due to ambient atmosphere and humidity exposure calculated from the peak areas of Fig. 5.

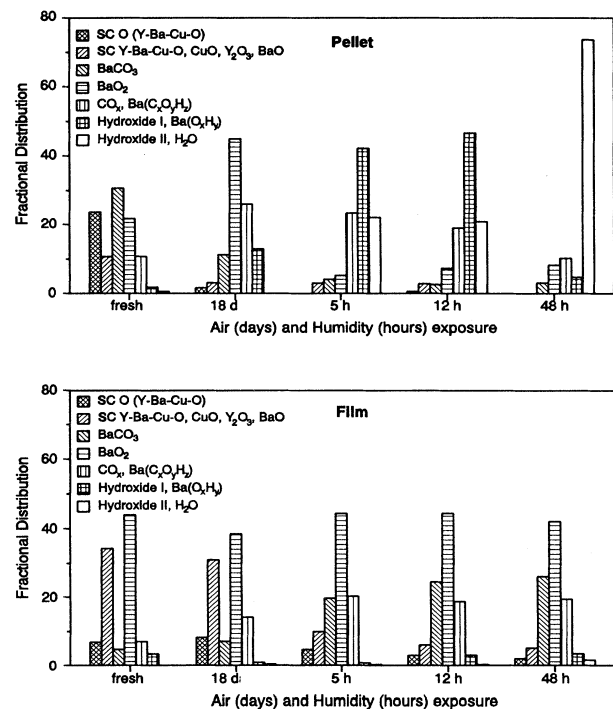


FIG. 8. Change in the O  $1s$  XPS peak due to ambient atmosphere and humidity exposure calculated from the peak areas of Fig. 6.

and XPS data show a significant Cu concentration at the film surface in contrast to the pellet which has none. Also, no excess Ba was present on the film surface. The nonsuperconducting cuprate phase is likely an oxygen-deficient structure ( $\text{YBa}_2\text{Cu}_3\text{O}_6$ ) (Refs. 22 and 41) which lost an oxygen and a Ba to form  $\text{BaCO}_3$  by picking up  $\text{CO}_2$  from the atmosphere.

These results are supported by the peak resolution of the O 1s spectra (Fig. 8) where large hydroxide peaks in the pellet sample become predominant upon exposure to humid environments while the superconducting Ba and O species are still measurable for the films. The carbonate peak is also present in the pellet, and the cuprate peaks vanish from the surface upon exposure to humid air.

### SUMMARY AND CONCLUSIONS

$\text{YBa}_2\text{Cu}_3\text{O}_{7-\delta}$  samples exposed to ambient air and humidity exhibit similarities and differences in behavior. The samples, which consist of sintered pellets and rf sputtered films, exhibit a loss of superconducting phase with exposure and a tendency to form carbonate species in ambient air and hydrate and hydroxide species in humid air. Both types of samples exhibit a large excess of surface Ba and a depletion in Cu. However, the Cu surface concentration of the pellet vanishes with exposure to 85% relative humidity at 50°C over 48 h while the film still manages to retain a significant portion of its initial sur-

face Cu concentration. While the pellet exhibits a surface primarily covered with carbonate and hydroxide species, the film is primarily covered by a nonsuperconducting barium cuprate phase, most likely oxygen deficient. Differences in severity of degradation between these two samples and also between high-porosity pellets and laser-ablated films, which exhibited even more severe degradation, indicate that the rate-controlling process in the environmental attack of  $\text{YBa}_2\text{Cu}_3\text{O}_{7-\delta}$  superconducting perovskites occurs by Ba diffusion to the surface and Cu depletion from the surface through the grain boundary. Thus samples with fine grains and a small grain-boundary volume exhibit a good resistance to environmental degradation (i.e., the rf sputtered films), while samples with larger grains and greater grain-boundary volume are very susceptible to phase changes and chemical reactions in a thick region below the surface (pellets exhibited a transformed layer about 600 nm thick after only 48 h of exposure to humid air).

### ACKNOWLEDGMENTS

The authors wish to thank Paul Holloway for valuable discussions, Eric Lambers for help with SAM data, Greg Chandler for fabricating the  $\text{YBa}_2\text{Cu}_3\text{O}_{7-\delta}$  pellets, and Kelly Truman and Carl Mueller for fabricating the film samples. This research was funded by DARPA under Contract No. MDA 972-88-J-1006.

- <sup>1</sup>M. F. Yan, R. L. Barns, H. M. O'Bryan, Jr., P. K. Gallagher, R. C. Sherwood, and S. Jin, *Appl. Phys. Lett.* **51**, 532 (1987).
- <sup>2</sup>A. Sequeira, H. Rajagopal, and J. V. Yakhmi, *Solid State Commun.* **65**, 991 (1988).
- <sup>3</sup>S. L. Qui, M. W. Ruckman, N. B. Brookes, P. D. Johnson, J. Chen, C. L. Lin, B. Sinković, and M. Strongin, *Phys. Rev. B* **37**, 3747 (1988).
- <sup>4</sup>S. L. Qui, C. L. Lin, M. W. Ruckman, J. Chen, D. H. Chen, Y. Xu, A. R. Moodenbaugh, M. Strogin, D. Nichols, and J. E. Crow, in *High- $T_c$  Superconducting Thin Films, Devices, and Applications*, Proceedings of the 1988 topical conference on High- $T_c$  Superconducting Thin Films, Devices, and Applications of the AVS held in Atlanta, GA, October, 1988, AIP Conf. Proc. No. 182, edited by G. Margaritondo, R. Joynt, and M. Onellion (AIP, New York, 1989), p. 368.
- <sup>5</sup>H. W. Zandbergen, R. Gronsky, and G. Thomas, *Phys. Status Solidi A* **105**, 207 (1988).
- <sup>6</sup>J. G. Thompson, B. G. Hyde, R. L. Withers, J. S. Anderson, J. G. Fitz Gerald, J. Bitmead, M. S. Paterson, and A. M. Steward, *Mater. Res. Bull.* **22**, 1715 (1987).
- <sup>7</sup>V. I. Nefedov, A. N. Sokolov, M. A. Tyzykhov, N. N. Oleinikov, Ye. A. Yeremina, and M. A. Kolotyrykina, *J. Electron Spectrosc. Relat. Phenom.* **49**, 47 (1989).
- <sup>8</sup>L. D. Fitch and V. L. Burdick, *J. Am. Ceram. Soc.* **72**, 2020 (1989).
- <sup>9</sup>B. G. Hyde, J. G. Thompson, R. L. Withers, J. G. Fitz Gerald, A. M. Steward, D. J. M. Bevan, J. S. Anderson, J. Bitmead, and M. S. Paterson, *Nature* **327**, 402 (1987).
- <sup>10</sup>N. M. Hwang, G. W. Bahng, Y. K. Park, J. C. Park, H. G. Moon, and D. N. Yoon, *J. Mater. Sci. Lett.* **8**, 517 (1989).
- <sup>11</sup>L. B. Harris and F. K. Nyang, *Solid State Commun.* **67**, 359 (1988).
- <sup>12</sup>H.-X. Liu, D. L. Cocke, D. G. Naugle, and R. K. Pandey, *Solid State Ionics* **32/33**, 1125 (1989).
- <sup>13</sup>M. W. Ruckman, S. M. Herald, D. DiMarzio, H. Chen, A. R. Moodenbaugh, and C. Y. Yang, in *High- $T_c$  Superconducting Thin Films, Devices, and Applications* (Ref. 4), p. 360.
- <sup>14</sup>S. Myhra, J. C. Riviere, A. M. Steward, and P. C. Healy, *Z. Phys. B* **72**, 413 (1988).
- <sup>15</sup>F. Stucki, P. Brüesch, and Th. Baumann, *Physica C* **156**, 461 (1988).
- <sup>16</sup>W. K. Ford, J. Anderson, G. V. Rubenacker, J. E. Drumheller, C. T. Chen, M. Hong, J. Kwo, and S. H. Liou, *J. Mater. Res.* **4**, 16 (1989); W. K. Ford, C. T. Chen, J. Anderson, M. Hong, J. Kwo, S. H. Liou, G. V. Rubenacker, and J. E. Drumheller, *Phys. Rev. B* **37**, 7924 (1988).
- <sup>17</sup>D. Van der Marel, J. van Elp, G. A. Sawatzky, and D. Heitmann, *Phys. Rev. B* **37**, 5136 (1988).
- <sup>18</sup>N. G. Stoffel, P. A. Morris, W. A. Bonner, D. LaGraffe, M. Tang, Y. Chang, G. Margaritondo, and M. Onellion, *Phys. Rev. B* **38**, 213 (1988).
- <sup>19</sup>I. Ahmad, G. T. Chandler, and D. E. Clark, *Mater. Res. Soc. Symp. Proc.* **124**, 239 (1988).
- <sup>20</sup>K. Truman, Ph. D. dissertation, University of Florida, 1991.
- <sup>21</sup>W. Herzog, M. Schwartz, H. Sixl, and R. Hoppe, *Z. Phys. B* **72**, 19 (1988).
- <sup>22</sup>J. Halbritter, P. Walk, H.-J. Mathes, B. Hauser, and H. Rogalla, *Z. Phys. B* **73**, 277 (1988).
- <sup>23</sup>P. Steiner, B. Kinsinger, I. Sander, B. Siegwart, S. Hüfner, and C. Politis, *Z. Phys. B* **67**, 19 (1987).

- <sup>24</sup>R. Caracciolo, M. S. Hedge, J. B. Wachtman, Jr., A. Inam, and T. Venkatesan, in *High- $T_c$  Superconducting Thin Films, Devices, and Applications* (Ref. 4), p. 232.
- <sup>25</sup>X. D. Wu, A. Inam, M. S. Hegde, T. Venkatesan, C. C. Chang, E. W. Chase, B. Wilkens, and J. M. Tarascon, *Phys. Rev. B* **38**, 9307 (1988).
- <sup>26</sup>H. Jaeger, S. Hofmann, G. Kaiser, K. Schulze, and P. Petzow, *Physica C* **153-155**, 133 (1988).
- <sup>27</sup>J. R. Gavaler and A. I. Braginski, *Physica C* **153-155**, 1435 (1988).
- <sup>28</sup>J. H. Thomas III and M. E. Labib, in *Thin Film Processing and Characterization of High-Temperature Superconductors*, Proceedings of the American Society Topical Conference on Thin Film Processing and Characterization of High- $T_c$  Superconductors, AIP Conf. Proc. No. 165, edited by J. M. E. Harper, J. Colton, and L. C. Feldman (AIP, New York, 1987), p. 374.
- <sup>29</sup>L. D. Marks, D. J. Li, H. Shibahara, and J. P. Zhang, *J. Electron Microsc. Technol.* **8**, 297 (1988).
- <sup>30</sup>D. D. Wagman, W. H. Evans, V. B. Parker, R. H. Schumm, S. M. Bailey, I. Halow, K. L. Churney, and R. L. Nuttall, in *Handbook of Chemistry and Physics*, 65th ed., edited by R. C. Weast (C.R.C. Boca Raton, FL, 1985), p. D53.
- <sup>31</sup>D. Majumdar, D. Chatterjee, and G. Pav-Pujalt, *Physica C* **158**, 413 (1989).
- <sup>32</sup>F. Stucki, P. Brüesch, and T. Baumann, *Physica C* **153-155**, 200 (1988).
- <sup>33</sup>J. W. Rogers, Jr., N. D. Shinn, J. E. Schirber, E. L. Venturini, D. S. Ginley, and B. Morosin, *Phys. Rev. B* **38**, 5021 (1988).
- <sup>34</sup>N. S. McIntyre, in *Practical Surface Analysis by Auger and X-Ray Photoelectron Spectroscopy*, edited by D. Briggs and M. P. Seah (Wiley, New York, 1983), p. 410.
- <sup>35</sup>H. Fjellvåg, P. Karen, A. Kjekshus, and J. K. Grepstad, *Acta Chem. Scand. A* **42**, 171 (1988).
- <sup>36</sup>F. Parmigiani, G. Chiarello, N. Ripamoni, H. Goretzki, and U. Roll, *Phys. Rev. B* **36**, 7148 (1987).
- <sup>37</sup>D. D. Sarma, K. Sreedhard, P. Ganguly, and C. N. R. Rao, *Phys. Rev. B* **36**, 2371 (1987); S. Kohiki, T. Hamada, and T. Wada, *ibid.* **36**, 2290 (1987).
- <sup>38</sup>T. Kachel, P. Sen, B. Dauth, and M. Campagna, *Z. Phys. B* **70**, 137 (1988).
- <sup>39</sup>P. M. A. Sherwood, in *Practical Surface Analysis by Auger and X-Ray Photoelectron Spectroscopy* (Ref. 34), p. 454.
- <sup>40</sup>J. A. T. Verhoeven and H. van Doveren, *Appl. Surf. Sci.* **5**, 361 (1980).
- <sup>41</sup>R. Liu, C. G. Olson, A. B. Yang, C. Gu, D. W. Lynch, A. J. Arko, R. S. List, R. J. Bartlett, B. W. Veal, J. Z. Liu, A. P. Paulikas, and K. Vandervoort, *Phys. Rev. B* **40**, 2650 (1989).